Representation theorems and Green's function retrieval for scattering in acoustic media

Ivan Vasconcelos,[1] Roel Snieder,[2] and Huub Douma[1]

[1]*ION Geophysical, GXT Imaging Solutions, 1st Floor, Integra House, Vicarage Road, Egham, Surrey TW20 9JZ, United Kingdom*
[2]*Center for Wave Phenomena, Department of Geophysics, Colorado School of Mines, Golden, Colorado 80401, USA*

Reciprocity theorems for perturbed acoustic media are provided in the form of convolution- and correlation-type theorems. These reciprocity relations are particularly useful in the general treatment of both forward and inverse-scattering problems. Using Green's functions to describe perturbed and unperturbed waves in two distinct wave states, representation theorems for scattered waves are derived from the reciprocity relations. While the convolution-type theorems can be manipulated to obtain scattering integrals that are analogous to the Lippmann-Schwinger equation, the correlation-type theorems can be used to retrieve the scattering response of the medium by cross correlations. Unlike previous formulations of Green's function retrieval, the extraction of scattered-wave responses by cross correlations does not require energy equipartitioning. Allowing for uneven energy radiation brings experimental advantages to the retrieval of fields scattered by remote lossless and/or attenuative scatterers. These concepts are illustrated with a number of examples, including analytic solutions to a one-dimensional scattering problem, and a numerical example in the context of seismic waves recorded on the ocean bottom.

I. INTRODUCTION

Reciprocity theorems have long been used to describe important properties of wave propagation phenomena. Rayleigh [1] used a local form of an acoustic reciprocity theorem to demonstrate source-receiver reciprocity. Time-domain reciprocity theorems were later generalized to relate two wave states with different field, material, and source properties in absorbing heterogeneous media [2].

Fokkema and van den Berg [3] showed that acoustic reciprocity theorems can be used for modeling wave propagation, for boundary and domain imaging, and for estimation of the medium properties. In the field of exploration seismology, an important application of convolution-type reciprocity theorems lies in removing multiple reflections, also called *multiples*, caused by the Earth's free surface [3,4]. These approaches rely on the convolution of single-scattered waves to create multiples, which are then adaptively subtracted from the recorded data. Other approaches for the elimination of multiples from seismic data rely on inverse-scattering methods [5]. The inverse-scattering-based methodologies are typically used separately from the representation[1] theorem approaches [3,4] in predicting multiples.

Recent forms of reciprocity theorems have been derived for the extraction of Green's functions [6,7], showing that the cross correlations of waves recorded by two receivers can be used to obtain the waves that propagate between these receivers as if one of them behaves as a source. These results coincide with other studies based on cross correlations of diffuse waves in a medium with an irregular boundary [8], caused by randomly distributed uncorrelated sources [9,10], or present in the coda of the recorded signals [11]. An early analysis by Claerbout [12] shows that the reflection response in a one-dimensional (1D) medium can be reconstructed

from the autocorrelation of recorded transmission responses. This result was later extended for cross correlations in heterogeneous three-dimensional media by Wapenaar *et al.* [13], who used one-way reciprocity theorems in their derivations. Green's function retrieval by cross correlations has found applications in the fields of global [10,14] and exploration seismology [15,16], ultrasonics [17,18], helioseismology [19], structural engineering [20,21], and ocean acoustics [22,23].

Although the ability to reconstruct the Green's function between two observation points via cross correlations has been shown for special cases by methods other than representation theorems (e.g., [8,16,24]), the derivations based on representation theorems have provided for generalizations beyond lossless acoustic wave propagation to elastic wave propagation and diffusion. More general forms of reciprocity relations have been derived [7,25,26] which include a wide range of differential equations such as the acoustic, elastodynamic, and electromagnetic wave equations, as well as the diffusion, advection, and Schrödinger equations, among others.

In this paper, we derive reciprocity theorems for acoustic perturbed media. The perturbations of the wave field due to the perturbation of the medium can be used for imaging or for monitoring. For imaging, the unperturbed medium is assumed to be so smooth that it does not generate reflected waves, while discontinuities in the perturbation account for scattering. In monitoring applications, the perturbation consists of the time-lapse changes in the medium. Although previous derivations of reciprocity theorems account for arbitrary medium parameters that are different between two wave states [2,3,7], they do not explicitly consider the special case of perturbed media or scattering. In perturbed media, there are special relations between the unperturbed and perturbed wave states (e.g., in terms of the physical excitation) that make the reciprocity theorems in such media differ in form with respect to their more general counterparts [3,7].

---

[1]Representation theorems are derived from reciprocity theorems using Green's functions; e.g., see Sec. III of this paper.

Here we focus on deriving and discussing some of these differences.

One particularly important aspect of studying scattering-based reciprocity lies in retrieving wave field perturbations from cross correlations [7,25]. As we show here, wave field perturbations by themselves do not satisfy the wave equations and thus their retrieval does not follow directly from earlier derivations. More importantly, here we demonstrate that the accurate retrieval of scattered waves by correlation does not require energy equipartitioning as does the retrieval of full-field responses [7,24,25]. This is an important result for dealing with certain remote sensing and imaging experiments where only a finite aperture of physical sources is available. Moreover, we show that this result holds both for lossless and attenuative scattering problems.

We first outline general forms of convolution- and correlation-type reciprocity theorems by manipulating the perturbed and unperturbed wave equations for two wave states. Then, we write the more general reciprocity relations as representation theorems using the Green's functions for unperturbed and perturbed waves in the two states. We show that the convolution-type theorem results in a familiar scattering integral that describes field perturbations between two observation points. Next we analyze how the correlation-type theorems can be used to extract the field perturbations from cross correlations of observed fields for different types of media and experimental configurations. Finally, we discuss the applications of these representation theorems in recovering the perturbation response between two sensors from random medium fluctuations and from coherent surface sources. Our results are illustrated by one-dimensional analytic examples and by a numerical example of the application of scattering reciprocity to acoustic waves recorded at the ocean bottom.

II. RECIPROCITY THEOREMS IN CONVOLUTION AND CORRELATION FORM

We define acoustic wave states in a domain $\mathbb{V} \subset \mathbb{R}^d$, bounded by $\partial \mathbb{V} \subset \mathbb{R}^d$ (Fig. 1). The outward pointing normal to $\partial \mathbb{V}$ is represented by $\mathbf{n}$. We consider two wave states, which we denote by the superscripts A and B, respectively. Each wave state is defined in an unperturbed medium with compressibility $\kappa_0(\mathbf{r})$ and density $\rho_0(\mathbf{r})$, as well as in a perturbed medium described by $\kappa(\mathbf{r})$ and $\rho(\mathbf{r})$. Using the Fourier convention $u(t) = \int u(\omega) \exp(-i\omega t) d\omega$, the field equations for state A in a perturbed medium are, in the frequency domain,

$$\boldsymbol{\nabla} p^A(\mathbf{r}, \omega) - i\omega \rho(\mathbf{r}) \mathbf{v}^A(\mathbf{r}, \omega) = 0,$$

$$\boldsymbol{\nabla} \cdot \mathbf{v}^A(\mathbf{r}, \omega) - i\omega \kappa(\mathbf{r}) p^A(\mathbf{r}, \omega) = q^A(\mathbf{r}, \omega), \quad (1)$$

where $p^A(\mathbf{r}, \omega)$ and $\mathbf{v}^A(\mathbf{r}, \omega)$ represent pressure and particle velocity, respectively, observed at the point $\mathbf{r} \in \mathbb{R}^d$ for a given time-harmonic frequency $\omega \in \mathbb{R}$. The perturbed fields for any wave state are $p = p_0 + p_S$ and $\mathbf{v} = \mathbf{v}_0 + \mathbf{v}_S$, where the subscript S indicates the wave field perturbation caused by medium changes. The quantity $q^A(\mathbf{r}, \omega)$ describes the source distribution as a volume injection rate density and is the same for both perturbed and unperturbed waves. Our nota-
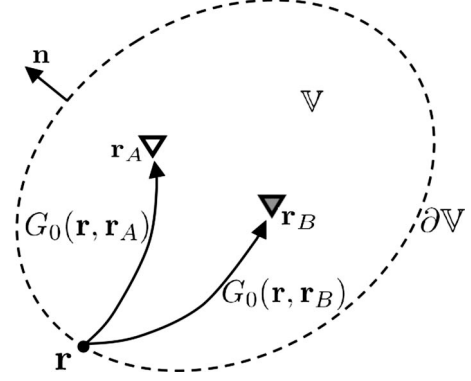

FIG. 1. Illustration of the domain used in the reciprocity theorems. The domain consists of a volume $\mathbb{V}$, bounded by $\partial \mathbb{V}$. The unit vector normal to $\partial \mathbb{V}$ is represented by $\mathbf{n}$. The wave states A and B are represented by receivers placed at $\mathbf{r}_A$ (white triangle) and $\mathbf{r}_B$ (gray triangle), respectively. The solid arrows denote the stationary paths of unperturbed waves G_0, propagating between the receivers and an arbitrary point $\mathbf{r}$ on $\partial \mathbb{V}$.

tion is such that $\boldsymbol{\nabla} = (\partial / \partial r_1, \ldots, \partial / \partial r_d)^T$ and $\boldsymbol{\nabla} \cdot \mathbf{v} = \sum_{i=1}^{d} \partial v_i / \partial r_i$. The unperturbed wave equations are obtained by adding the subscript 0 to coefficients and field quantities in Eq. (1).

We assume that no volume forces are present by setting the right-hand side (RHS) of the vector relation in Eq. (1) equals zero. For brevity, we assume that perturbations only occur in compressibility, thus $\rho = \rho_0$, but our derivations can be generalized to include density perturbation as well. We make no restrictions on the smoothness of the material parameters, i.e., rapid lateral changes and discontinuities are allowed.

To derive Rayleigh's reciprocity theorem [1–3], we insert the equations of motion and stress-strain relations for states A and B in

$$\mathbf{v}_0^B \cdot \mathbf{E}_0^A + p_0^A E_0^B - \mathbf{v}_0^A \cdot \mathbf{E}_0^B - p_0^B E_0^A, \quad (2)$$

where $\mathbf{E}$ and E represent, from Eq. (1), the equation of motion (first line of the equation) and the stress-strain relation (second line of the equation), respectively. For brevity, we omit the parameter dependence on $\mathbf{r}$ and ω. From Eq. (2) we isolate the *interaction quantity* $\boldsymbol{\nabla} \cdot (p_0^A \mathbf{v}_0^B - p_0^B \mathbf{v}_0^A)$ [2]. Next, we integrate the result of Eq. (2) over the domain $\mathbb{V}$ and apply Gauss' divergence theorem. This results in

$$\oint_{\mathbf{r} \in \partial \mathbb{V}} [p_0^A \mathbf{v}_0^B - p_0^B \mathbf{v}_0^A] \cdot d\mathbf{S} = \int_{\mathbf{r} \in \mathbb{V}} [p_0^A q_0^B - p_0^B q_0^A] dV, \quad (3)$$

which is referred to as a reciprocity theorem of the convolution type [2,3] because the frequency-domain products of field parameters represent convolutions in the time domain. A correlation-type reciprocity theorem [2,3] can be derived from isolating the interaction quantity $\boldsymbol{\nabla} \cdot (p_0^A \mathbf{v}_0^{B*} + p_0^{B*} \mathbf{v}_0^A)$ from

$$\mathbf{v}_0^{B*} \cdot \mathbf{E}_0^A + p_0^A E_0^{B*} + \mathbf{v}_0^A \cdot \mathbf{E}_0^{B*} + p_0^{B*} E_0^A, \tag{4}$$

where superscript $*$ denotes complex conjugation. Subsequent volume integration and application of the divergence theorem yield

$$\oint_{\mathbf{r} \in \partial \mathbb{V}} [p_0^A \mathbf{v}_0^{B*} + p_0^{B*} \mathbf{v}_0^A] \cdot d\mathbf{S} = \int_{\mathbf{r} \in \mathbb{V}} [p_0^A q_0^{B*} + p_0^{B*} q_0^A] dV, \tag{5}$$

where complex conjugates translate into time-domain cross correlations of field parameters. For this reason, Eq. (5) is a reciprocity theorem of the correlation type [2,3]. Convolution- and correlation-type reciprocity theorems for the perturbed wave states [e.g., Eq. (1)] can be expressed simply by removing the subscript 0 from Eqs. (2)–(5). In Eq. (5) we assume that κ_0 and ρ_0 are real quantities (i.e., the medium is lossless).

The theorems in Eqs. (3) and (5) hold when the material properties in states A and B are the same. General reciprocity theorems that account for arbitrarily different source and material properties between two wave states have been derived in [2,3]. Here, we further develop these reciprocity theorems for the special case of perturbed acoustic media. First, we isolate $\boldsymbol{\nabla} \cdot (p^A \mathbf{v}_0^B - p_0^B \mathbf{v}^A)$ from

$$\mathbf{v}_0^B \cdot \mathbf{E}^A + p^A E_0^B - \mathbf{v}^A \cdot \mathbf{E}_0^B - p_0^B E^A. \tag{6}$$

After separating this quantity, we integrate over $\mathbf{r} \in \mathbb{V}$ and apply the divergence theorem. Using $p = p_0 + p_S$ and $\mathbf{v} = \mathbf{v}_0 + \mathbf{v}_S$ and subtracting Eq. (3), we obtain

$$\oint_{\mathbf{r} \in \partial \mathbb{V}} [p_S^A \mathbf{v}_0^B - p_0^B \mathbf{v}_S^A] \cdot d\mathbf{S} = \int_{\mathbf{r} \in \mathbb{V}} p_S^A q_0^B dV$$
$$+ \int_{\mathbf{r} \in \mathbb{V}} i\omega(\kappa_0 - \kappa) p^A p_0^B dV, \tag{7}$$

which is a convolution-type reciprocity theorem for perturbed media.

The correlation-type counterpart of Eq. (7) can be derived from the interaction quantity $\boldsymbol{\nabla} \cdot (p^A \mathbf{v}_0^{B*} + p_0^{B*} \mathbf{v}^A)$, which can be isolated from

$$\mathbf{v}_0^{B*} \cdot \mathbf{E}^A + p^A E_0^{B*} + \mathbf{v}^A \cdot \mathbf{E}_0^{B*} + p_0^{B*} E^A. \tag{8}$$

After performing the same steps as in the derivation of Eq. (7) we obtain

$$\oint_{\mathbf{r} \in \mathbb{V}} [p_S^A \mathbf{v}_0^{B*} + p_0^{B*} \mathbf{v}_S^A] \cdot d\mathbf{S} = \int_{\mathbf{r} \in \mathbb{V}} p_S^A q_0^{B*} dV$$
$$- \int_{\mathbf{r} \in \mathbb{V}} i\omega(\kappa_0 - \kappa) p^A p_0^{B*} dV, \tag{9}$$

which is a correlation-type reciprocity theorem for perturbed acoustic media. Again, we assume that both κ and κ_0 are real (i.e., no attenuation).

By interchanging the superscripts in Eqs. (6) and (8) we derive convolution- and correlation-type reciprocity theorems that relate the perturbations p_S^B and $\mathbf{v}_S^B$ to p_0^A and $\mathbf{v}_0^A$. These theorems have the same form as the ones in Eqs. (7) and (9), except A is interchanged with B in Eq. (7) and with $B*$ in Eq. (9). Although Eqs. (7) and (8) account for compressibility changes only, they can be modified to include density perturbations. Such modification involves adding, to the RHS of the equations, an extra volume integral whose integrand is proportional to $(\rho_0 - \rho)$ and the wave fields $\mathbf{v}^A$ and $\mathbf{v}_0^B$ (or $\mathbf{v}_0^{B*}$) [3].

III. SCATTERING-BASED REPRESENTATIONS AND APPLICATIONS

We introduce the Green's functions, in the frequency domain, by setting

$$q^{A,B} = \delta(\mathbf{r} - \mathbf{r}_{A,B}), \quad \mathbf{r}_{A,B} \in \mathbb{R}^d. \tag{10}$$

This choice for q allows for expressing the field quantity p in terms of the Green's functions G, i.e.,

$$p^{A,B}(\mathbf{r}, \omega) = G(\mathbf{r}_{A,B}, \mathbf{r}, \omega) = G_0(\mathbf{r}_{A,B}, \mathbf{r}, \omega) + G_S(\mathbf{r}_{A,B}, \mathbf{r}, \omega). \tag{11}$$

Note that these are the Green's functions for sources of the volume injection rate type. The derivation below can also be reproduced using volume forces [6]. It follows from Eqs. (11) and (1) that $\mathbf{v}^{A,B}(\mathbf{r}, \omega) = (i\omega\rho)^{-1} \boldsymbol{\nabla} G(\mathbf{r}_{A,B}, \mathbf{r}, \omega)$.

Using these definitions, the convolution-type theorem in Eq. (7) becomes

$$G_S(\mathbf{r}_A, \mathbf{r}_B) = \int_{\mathbf{r} \in \mathbb{V}} G_S(\mathbf{r}_A, \mathbf{r}) \delta(\mathbf{r} - \mathbf{r}_B) dV$$
$$= \oint_{\mathbf{r} \in \partial \mathbb{V}} \frac{1}{i\omega\rho} [G_S(\mathbf{r}_A, \mathbf{r}) \boldsymbol{\nabla} G_0(\mathbf{r}_B, \mathbf{r})$$
$$- G_0(\mathbf{r}_B, \mathbf{r}) \boldsymbol{\nabla} G_S(\mathbf{r}_A, \mathbf{r})] \cdot d\mathbf{S}$$
$$+ \int_{\mathbf{r} \in \mathbb{V}} \frac{1}{i\omega\rho} G(\mathbf{r}_A, \mathbf{r}) \mathcal{V}(\mathbf{r}) G_0(\mathbf{r}_B, \mathbf{r}) dV, \tag{12}$$

where $\mathcal{V}(\mathbf{r}) = \rho\omega^2 [\kappa(\mathbf{r}) - \kappa_0(\mathbf{r})]$ is the *perturbation operator* or *scattering potential* [27]. For brevity we omit the dependence on the frequency ω. Now we consider this equation under homogeneous boundary conditions on $\partial\mathbb{V}$, namely, (i) Sommerfeld radiation conditions [6], (ii) Dirichlet boundary conditions, i.e., $G_{0,S}(\mathbf{r}, \mathbf{r}_{A,B}) = 0 \ \ \forall \mathbf{r} \in \partial\mathbb{V}$, and/or (iii) Neumann boundary conditions, $\boldsymbol{\nabla} G_{0,S}(\mathbf{r}, \mathbf{r}_{A,B}) \cdot \mathbf{n} = 0 \ \ \forall \mathbf{r} \in \partial\mathbb{V}$. This gives

$$G_S(\mathbf{r}_A, \mathbf{r}_B) = \int_{\mathbf{r} \in \mathbb{V}} \frac{1}{i\omega\rho} G(\mathbf{r}_A, \mathbf{r}) \mathcal{V}(\mathbf{r}) G_0(\mathbf{r}_B, \mathbf{r}) dV. \tag{13}$$
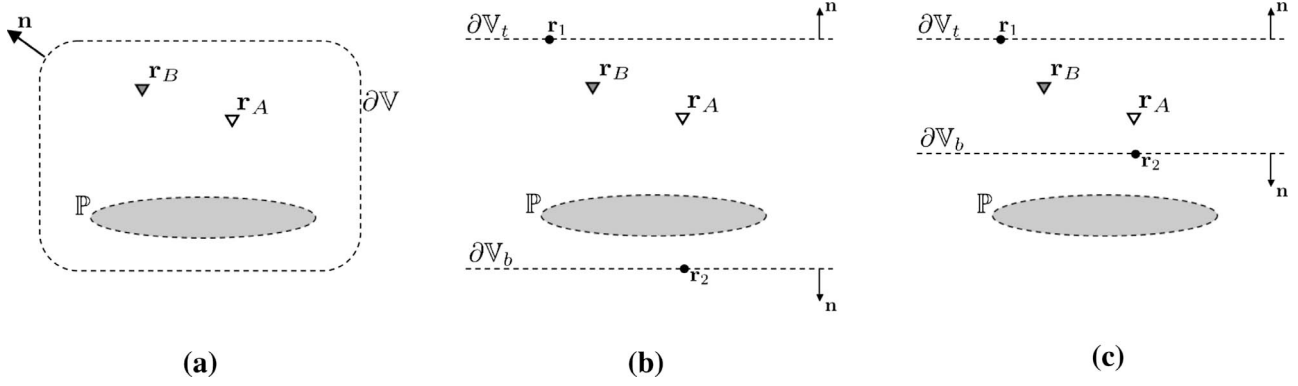
FIG. 2. Schematic illustrations of configurations for case I. Medium perturbations are restricted to the subdomain $\mathbb{P}$, which is placed away from the observation points. By infinitely extending the sides of $\partial\mathbb{V}$, the closed surface integral can be replaced by an integral over $\mathbf{r} \in \partial\mathbb{V}_b \cup \partial\mathbb{V}_t$, as portrayed in panels (a) and (b). In our discussion, we fix the sets $\partial\mathbb{V}_t$ and $\mathbb{P}$ and have two choices for $\partial\mathbb{V}_b$ such that in (b) $\mathbb{P} \subset \mathbb{V}$ and in (c) $\mathbb{P} \not\subset \mathbb{V}$.

Equation (13) is the integral equation known as the *Lippmann-Schwinger* equation [27], commonly used for modeling and inversion or imaging in scattering problems. When none of the surface boundary conditions listed above apply, the surface integral of Eq. (7) should be added to the right-hand side of Eq. (13).

Next, we turn our attention to the correlation-type reciprocity theorem in Eq. (9). Substituting the Green's functions [Eq. (11)] for the wave fields p and $\mathbf{v}$ in Eq. (9) gives

$$
\begin{aligned}
G_S(\mathbf{r}_A, \mathbf{r}_B) &= \int_{\mathbf{r} \in \mathbb{V}} G_S(\mathbf{r}_A, \mathbf{r}) \delta(\mathbf{r} - \mathbf{r}_B) dV \\
&= \oint_{\mathbf{r} \in \partial\mathbb{V}} \frac{1}{i\omega\rho} [G_0^*(\mathbf{r}_B, \mathbf{r}) \, \boldsymbol{\nabla} \, G_S(\mathbf{r}_A, \mathbf{r}) \\
&\quad - G_S(\mathbf{r}_A, \mathbf{r}) \, \boldsymbol{\nabla} \, G_0^*(\mathbf{r}_B, \mathbf{r})] \cdot d\mathbf{S} \\
&\quad + \int_{\mathbf{r} \in \mathbb{V}} \frac{1}{i\omega\rho} G(\mathbf{r}_A, \mathbf{r}) \mathcal{V}(\mathbf{r}) G_0^*(\mathbf{r}_B, \mathbf{r}) dV. \quad (14)
\end{aligned}
$$

The surface integral here does not vanish under a Sommerfeld radiation condition, but with Dirichlet and/or Neumann boundary conditions we get

$$
G_S(\mathbf{r}_A, \mathbf{r}_B) = \int_{\mathbf{r} \in \mathbb{V}} \frac{1}{i\omega\rho} G(\mathbf{r}_A, \mathbf{r}) \mathcal{V}(\mathbf{r}) G_0^*(\mathbf{r}_B, \mathbf{r}) dV, \quad (15)
$$

which is similar to the Lippmann-Schwinger integral in Eq. (13), except for the complex conjugate in the RHS. Under Neumann and/or Dirichlet boundary conditions, inspection of Eqs. (13) and (15) states that modeling and inversion or imaging of scattered fields can be accomplished equally by

taking either time-advanced [i.e., $G_0(\mathbf{r}_B, \mathbf{r})$; Eq. (13)] or time-reversed [i.e., $G_0^*(\mathbf{r}_B, \mathbf{r})$; Eq. (15)] fields.

The left-hand side of Eq. (14) describes causal wave field perturbations that propagate from $\mathbf{r}_B$ to $\mathbf{r}_A$ as if the observation point at $\mathbf{r}_B$ acts as a source. By taking Eq. (14), interchanging subscripts A by $B*$, and taking the complex conjugate, we obtain

$$
\begin{aligned}
G_S^*(\mathbf{r}_A, \mathbf{r}_B) &= \oint_{\mathbf{r} \in \partial\mathbb{V}} \frac{1}{i\omega\rho} [G_S^*(\mathbf{r}_B, \mathbf{r}) \, \boldsymbol{\nabla} \, G_0(\mathbf{r}_A, \mathbf{r}) \\
&\quad - G_0(\mathbf{r}_A, \mathbf{r}) \, \boldsymbol{\nabla} \, G_S^*(\mathbf{r}_B, \mathbf{r})] \cdot d\mathbf{S} \\
&\quad - \int_{\mathbf{r} \in \mathbb{V}} \frac{1}{i\omega\rho} G^*(\mathbf{r}_B, \mathbf{r}) \mathcal{V}(\mathbf{r}) G_0(\mathbf{r}_A, \mathbf{r}) dV. \quad (16)
\end{aligned}
$$

There are two important differences between Eqs. (14) and (16) and previous expressions for Green's function retrieval [7,25]. The first difference is that here we obtain the wave field perturbations G_S, which by themselves do not satisfy the acoustic wave equations [e.g., Eq. (1)], from cross correlations of G_S with G_0. Second, the proper manipulation of unperturbed waves G_0 and perturbations G_S in the integrands of Eqs. (14) and (16) allows for the separate retrieval of causal and anticausal wave field perturbations $G_S(\mathbf{r}_A, \mathbf{r}_B)$ in the frequency domain rather than their superposition. Since the correlation-type representation theorems for G or G_0 [7,25] result in the superposition of causal and anticausal responses in the frequency domain, their time-domain counterparts retrieve *two sides* of the signal, i.e., they retrieve the wave field at both positive and negative times. Because of this, we refer to the theorems in Refs. [7,25] as *two-sided theorems*. The theorems in Eqs. (14) and (16) recover the time-domain field perturbation response for either positive [Eq. (14)] or negative [Eq. (16)] times only. Therefore, we call the theorems in Eqs. (14) and (16) *one-sided theorems*.

Let us consider a first scenario, which we refer to as *case I* (Fig. 2), defined by

(i) $\mathcal{V}(\mathbf{r}) \neq 0$;   only for $\mathbf{r} \in \mathbb{P}$; $\mathbb{P} \subset \mathbb{R}^d$

(ii) sing supp$[\mathcal{V}(\mathbf{r})] \neq 0$;   (i.e., $\mathcal{V}$ generates backscattering)

(iii) $\mathbf{r}_B \notin \mathbb{P}$;   (i.e., perturbations away from receiver acting as source)

(iv) $\kappa_0(\mathbf{r})$, $\rho_0(\mathbf{r}) \in C^\infty(\mathbb{R}^d)$;   (i.e., smooth background),   (17)

(v) $[iG_0(\mathbf{r},\mathbf{r}_s)]^{-1}\boldsymbol{\nabla}G_0(\mathbf{r},\mathbf{r}_s)\cdot\mathbf{n}(\mathbf{r}_s) > 0$; for $(\mathbf{r},\mathbf{r}_s) \in \partial\mathbb{V}_b$ or $\partial\mathbb{V}_t$ (i.e., outgoing reference waves)

$[iG_S(\mathbf{r},\mathbf{r}_s)]^{-1}\boldsymbol{\nabla}G_S(\mathbf{r},\mathbf{r}_s)\cdot\mathbf{n}(\mathbf{r}_s) < 0$; for $(\mathbf{r},\mathbf{r}_s) \in \partial\mathbb{V}_b$ (i.e., ingoing scattered waves).

In this case, Eq. (14) becomes

$$G_S(\mathbf{r}_A,\mathbf{r}_B) = \int_{\mathbf{r}\in(\partial\mathbb{V}_b\cup\partial\mathbb{V}_t)} \frac{1}{i\omega\rho}$$
$$\times[G_0^*(\mathbf{r}_B,\mathbf{r})\,\boldsymbol{\nabla}\,G_S(\mathbf{r}_A,\mathbf{r})$$
$$- G_S(\mathbf{r}_A,\mathbf{r})\,\boldsymbol{\nabla}\,G_0^*(\mathbf{r}_B,\mathbf{r})]\cdot d\mathbf{S}$$
$$+ \int_{\mathbf{r}\in\mathbb{P}} \frac{1}{i\omega\rho}G(\mathbf{r}_A,\mathbf{r})\mathcal{V}(\mathbf{r})G_0^*(\mathbf{r}_B,\mathbf{r})dV, \quad (18)$$

assuming that $\mathbb{P} \subset \mathbb{V}$ [Fig. 2(b)]. Note here that the integration is now carried out for sources on the open top surface $\partial\mathbb{V}_t$ and on the bottom surface $\partial\mathbb{V}_b$ (Fig. 2). If $\mathbb{P} \not\subset \mathbb{V}$ [Fig. 2(c)], then $\mathcal{V}(\mathbf{r})=0$ $\forall\mathbf{r}\in\mathbb{V}$, which results in

$$\int_{\mathbf{r}\in\mathbb{V}} \frac{1}{i\omega\rho}G(\mathbf{r}_A,\mathbf{r})\mathcal{V}(\mathbf{r})G_0^*(\mathbf{r}_B,\mathbf{r})dV = 0. \quad (19)$$

Furthermore, if $\mathbb{P}\not\subset\mathbb{V}$ as in Fig. 2(c), $[iG_0^*(\mathbf{r},\mathbf{r}_s)]^{-1}\boldsymbol{\nabla}G_0^*(\mathbf{r}_B,\mathbf{r})\cdot\mathbf{n}<0$ and $[iG_S^*(\mathbf{r},\mathbf{r}_s)]^{-1}\boldsymbol{\nabla}G_S(\mathbf{r}_A,\mathbf{r})$ $\cdot\mathbf{n}>0$ for all $\mathbf{r}\in\partial\mathbb{V}_b$ [see conditions in Appendix A and Eq. (17)], giving

$$\int_{\mathbf{r}\in\partial\mathbb{V}_b} \frac{1}{i\omega\rho}[G_0^*(\mathbf{r}_B,\mathbf{r})\,\boldsymbol{\nabla}\,G_S(\mathbf{r}_A,\mathbf{r}) - G_S(\mathbf{r}_A,\mathbf{r})\,\boldsymbol{\nabla}\,G_0^*(\mathbf{r}_B,\mathbf{r})]\cdot d\mathbf{S}$$
$$= 0, \quad (20)$$

because the effective contributions of the two integral terms cancel (i.e., at the stationary points, both terms have the same phase and opposite polarity). This is addressed in detail in Appendix A. Therefore, using Eqs. (19) and (20) in Eq. (18), we have

$$G_S(\mathbf{r}_A,\mathbf{r}_B) = \int_{\mathbf{r}\in\partial\mathbb{V}_t} \frac{1}{i\omega\rho}[G_S(\mathbf{r}_A,\mathbf{r})\,\boldsymbol{\nabla}\,G_0^*(\mathbf{r}_B,\mathbf{r})$$
$$+ G_0^*(\mathbf{r}_B,\mathbf{r})\,\boldsymbol{\nabla}\,G_S(\mathbf{r}_A,\mathbf{r})]\cdot d\mathbf{S}. \quad (21)$$

Since this equation is not affected by any changes to $\partial\mathbb{V}_b$, this result is *equally valid* for $\mathbb{P} \subset \mathbb{V}$ as in Fig. 2(b). This is one of the key results in this paper. For $\mathbb{P} \subset \mathbb{V}$, the results in Eqs. (19) and (20) do not hold; by inserting Eq. (21) in Eq. (18) we obtain the identity

$$\int_{\mathbf{r}\in\partial\mathbb{V}_b} \frac{1}{i\omega\rho}[G_0^*(\mathbf{r}_B,\mathbf{r})\,\boldsymbol{\nabla}\,G_S(\mathbf{r}_A,\mathbf{r}) - G_S(\mathbf{r}_A,\mathbf{r})\,\boldsymbol{\nabla}\,G_0^*(\mathbf{r}_B,\mathbf{r})]\cdot d\mathbf{S}$$
$$= -\int_{\mathbf{r}\in\mathbb{V}} \frac{1}{i\omega\rho}G(\mathbf{r}_A,\mathbf{r})\mathcal{V}(\mathbf{r})G_0^*(\mathbf{r}_B,\mathbf{r})dV. \quad (22)$$

In case I [Figs. 2(b) and 2(c)], it follows from Eq. (21) that we can retrieve the exact scattered field $G_S(\mathbf{r}_A,\mathbf{r}_B)$ between two sensors by cross-correlating reference and scattered waves only from sources on the open top surface $\partial\mathbb{V}_t$. Moreover, Eqs. (19), (20), and (22) demonstrate that the volume integral in Eq. (18) exists only to account for medium perturbations that lie between surface sources and the receiver that acts as a pseudosource (i.e., $\mathbf{r}_B$ in this case). Therefore, in any practical configuration of case I, the bottom-surface sources and the volume integral can simply be neglected. This also implies that the observation points $\mathbf{r}_A$ could be anywhere (even inside $\mathbb{P}$). We illustrate how this observation holds for different source-receiver configurations with one-dimensional analytic examples (see below).

In general, the volume integrals in Eq. (14) cannot be ignored. Let us consider another example, *case II*, illustrated by Fig. 3. The configuration is similar to that of case I [see conditions in Eq. (17)], but now condition (iii) in Eq. (17) is modified to $\mathbf{r}_B \in \mathbb{P}$. So for case II, it is impossible to find source positions on $\partial\mathbb{V}$ for which there are waves whose
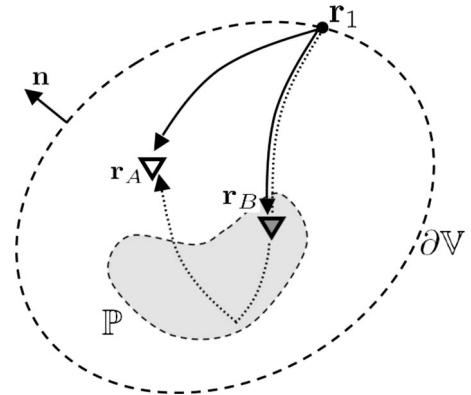

FIG. 3. Cartoon illustrating case II. The medium configuration in this case is the same as for case I (Fig. 2), but now one of the receivers at $\mathbf{r}_B$ is placed inside the perturbation volume $\mathbb{P}$. Solid arrows illustrate stationary paths of reference waves and the dashed arrow illustrates the path of a scattered wave. Here $\mathbf{r}_1$ illustrates a source position that yields a stationary contribution to the integrand in Eq. (21).
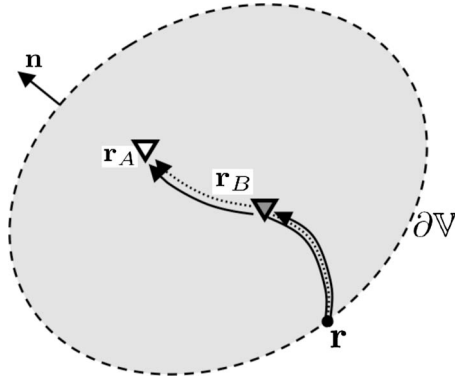
FIG. 4. Schematic representation of case III, where $\mathbb{P} \subseteq \mathbb{V}$, i.e., the medium perturbation occupies all of the volume $\mathbb{V}$. As in Fig. 2, solid and dashed arrows denote unperturbed waves and field perturbations, respectively.

paths, prescribed by reference waves, are not affected by the medium perturbation. Therefore, all integrals in Eq. (14) must always be evaluated. Another such example is *case III* in Fig. 4, where the perturbations occur over the entire volume, i.e., $\mathbb{P} \subseteq \mathbb{V}$ [see condition (i) in Eq. (17)].

IV. ANALYTIC EXAMPLE: 1D LAYERED MEDIA

As an example of case I [Fig. 2; defined via Eq. (17)] we present an acoustic one-dimensional model (Fig. 5) with a constant wave speed c_0 and wave number k_0, except in a layer of thickness H where the wave number is given by k_1. This defines $\mathbb{V} = \{z \in \mathbb{R}^1 | z \in [z_-, z_+]\}$, $\mathbb{P} = \{z \in \mathbb{R}^1 | z \in [0, H]\}$, and $\mathcal{V}(z) = k_0^2 - k^2 \quad \forall z \in \mathbb{P}$. It follows from the field equations [e.g., Eq. (1)] that for a 1D model with constant mass density ρ the pressure satisfies

$$\frac{d^2 p}{dz^2} + \kappa \rho \omega^2 p = i\omega \rho q, \quad z \in \mathbb{R}^1, \quad p \in \mathbb{C}^1. \quad (23)$$
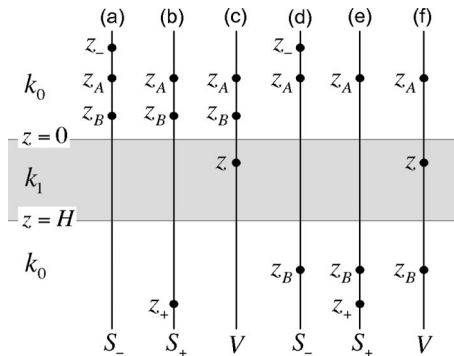
In this wave equation κ is given by

FIG. 5. Location of the receiver coordinates z_A and z_B and the source coordinates for the example of the one-layer model. This being a one-dimensional example of case I (Fig. 2), the medium perturbation (in gray shading) is compactly supported in the interval $[0, H]$ where the jump in wave number is given by $k_1 - k_0$. S_-, S_+, and V denote the 1D contributions of the top source, bottom source, and line integral, respectively. The three leftmost vertical lines represent the case where both receivers lie above the perturbations, while panels (d)–(f) denote the case where there is a receiver on either side of the perturbation.

$$\kappa = \frac{1}{\rho c^2} = \frac{k^2}{\rho \omega^2}. \quad (24)$$

For a homogeneous 1D medium with wave number k_0 the Green's function solution of expression (23) is given by

$$G_0(z, z_0) = \frac{\rho c_0}{2} e^{ik_0|z-z_0|}. \quad (25)$$

For the particular case of a 1D medium, the surface integral in Eq. (18) reduces to two end point contributions and the volume integral becomes a line integral. With Eq. (24), Eq. (18) under conditions set by Eq. (17) is given in one dimension by

$$G_S(z_A, z_B) = S_-(z_A, z_B) + S_+(z_A, z_B) + V(z_A, z_B), \quad (26)$$

with $S_-(r_B, r_A)$ as the contribution of a source above the receivers,

$$S_-(z_A, z_B) = \frac{2}{\rho c_0} G_S(z_A, z_-) G_0^*(z_B, z_-), \quad (27)$$

$S_+(z_A, z_B)$ as the contribution of a source below the receivers,

$$S_+(z_A, z_B) = \frac{2}{\rho c_0} G_S(z_A, z_+) G_0^*(z_B, z_+), \quad (28)$$

and $V(z_A, z_B)$ as the 1D volume integral,

$$V(z_A, z_B) = \frac{i}{\rho \omega} \int_0^H (k_0^2 - k_1^2) G(z_A, z) G_0^*(z_B, z) dz. \quad (29)$$

The contributions of these different terms are sketched in Fig. 5.

We first consider the case in which the two receivers are located above the layer ($z_A < 0$, $z_B < 0$). The three contributions to the perturbed Green's function are sketched in panels (a)–(c) in Fig. 5. As shown in Appendix B the contribution from the source above the layer [Fig. 5, panel (a)] gives the perturbed Green's function,

$$S_-(z_A, z_B) = G_S(z_A, z_B). \quad (30)$$

This means that the contribution of this boundary point suffices to give the perturbed Green's function. Note that the perturbed Green's function accounts for all reverberations within the layer, as well as for the velocity change in the layer. This demonstrates, in one dimension, the result in Eq. (21). As with Eq. (21), the result in Eq. (30) holds regardless of where the bottom source z_+ is positioned, i.e., whether $\mathbb{P} \subset \mathbb{V}$ or $\mathbb{P} \not\subset \mathbb{V}$. It follows from a comparison of expressions (26) and (30) that the contributions of S_+ and V cancel,

$$S_+(z_A, z_B) + V(z_A, z_B) = 0. \quad (31)$$

We show in Appendix B that this equality is indeed satisfied for the one-layer system considered here. This, in turn, demonstrates the result in Eq. (22).

Next consider sources on opposite sides of the layer ($z_A < 0$, $z_B > H$) as sketched in panels (d)–(f) of Fig. 5. We show in Appendix B that now the source under the layer [panel (e) of Fig. 5] suffices to give the perturbed Green's function,

$$S_+(z_A, z_B) = G_S(z_A, z_B). \tag{32}$$

We show in Appendix B that now the contributions S_- and V cancel,

$$S_-(z_A, z_B) + V(z_A, z_B) = 0, \tag{33}$$

which is, of course, required by Eq. (26). This result is in fact the same as in Eq. (21) if only $\mathbf{r}_B$ were beneath $\mathbb{P}$ in Fig. 2(b) and then the contributing surface would be $\partial \mathbb{V}_b$ instead of $\partial \mathbb{V}_t$. Since z_B and z_A are now in opposite sides of $\mathbb{P}$, Eqs. (32) and (33) also demonstrate that the general results in Eqs. (21) and (22) hold regardless of the position of the observation points $\mathbf{r}_A$. It is interesting to note that the end point contribution S_- satisfies

$$S_-(z_A, z_B) \sim e^{-ik_0(z_A + z_B)}. \tag{34}$$

Note that a change in the choice of the coordinate system alters the phase of this term. This contribution therefore corresponds to an unphysical arrival with an arrival time that is determined by the average position of the receivers. In higher dimensions, this can also be observed by inspecting the volume terms in Eqs. (14) and (16). An improper cancellation of this contribution with the volume term V would lead to unphysical arrivals in the extracted perturbed Green's function. It has been noted earlier that an inadequate source distribution may lead to unphysical arrivals in the extracted Green's function [26,28,29].

V. RETRIEVING G_S FROM RANDOM SOURCES IN $\mathbb{V}$: ENERGY CONSIDERATIONS

Consider Eq. (15), i.e.,

$$G_S(\mathbf{r}_A, \mathbf{r}_B) = -\int_{\mathbf{r} \in \mathbb{V}} i\omega(\kappa_0 - \kappa) G(\mathbf{r}_A, \mathbf{r}) G_0^*(\mathbf{r}_B, \mathbf{r}) dV. \tag{35}$$

When Dirichlet and/or Neumann boundary conditions apply [see derivation of Eq. (15)], the pressure observed at any given observation point $\mathbf{r}_o$ is given by

$$p(\mathbf{r}_o) = \int G(\mathbf{r}_o, \mathbf{r}) q(\mathbf{r}) dV \tag{36}$$

and likewise for unperturbed waves. q is the source term in Eq. (1). Next we consider random uncorrelated sources distributed through space, such that

$$\langle q(\mathbf{r}_1, \omega) q^*(\mathbf{r}_2, \omega) \rangle = \Delta\kappa(\mathbf{r}_1, \omega) \delta(\mathbf{r}_1 - \mathbf{r}_2) |R(\omega)|^2, \quad \mathbf{r}_{1,2} \in \mathbb{R}^d, \tag{37}$$

where $\Delta\kappa = \kappa_0 - \kappa$ and $|R(\omega)|^2$ is the power spectrum of a random excitation function and $\langle \cdot \rangle$ denotes an ensemble average. Note from Eq. (37) that the source intensity is proportional to the local perturbation $\Delta\kappa$ [i.e., $\sim \mathcal{V}(\mathbf{r})$] at every source position. We then multiply Eq. (35) by $|R(\omega)|^2$ to obtain
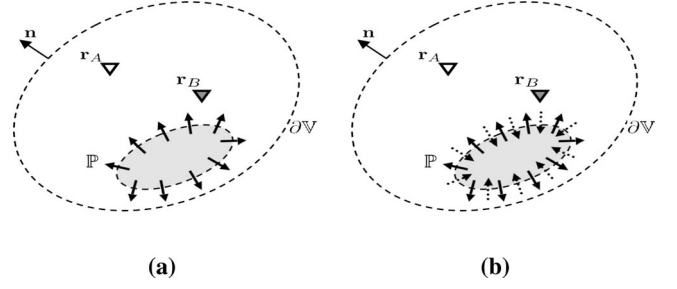

(a)   **(b)**

FIG. 6. Illustrations of energy considerations for extracting scattered waves from random volume sources in $\mathbb{V}$. To particularly highlight that equipartitioning is not a requirement for the retrieval of scattered waves; we use the medium configuration of case I (Fig. 2). Panel (a) represents the case where energy is purely out going (indicated by solid arrows) from $\mathbb{P}$; this is the case for scattering in lossless media or when Im$\{\mathcal{V}(\mathbf{r})\}$ and Im$\{\kappa_0(\mathbf{r})\}$ are nonzero only for $\mathbf{r} \in \mathbb{P}$. In the case of general attenuative materials, depicted in (b), where Im$\{\kappa_0(\mathbf{r})\} \neq 0$ $\forall \mathbf{r} \in \mathbb{V}$, there is an exchange of in- and out-going energies on the boundary $\partial \mathbb{P}$.

$$\begin{aligned} G_S(\mathbf{r}_A, \mathbf{r}_B) |R(\omega)|^2 = &-i\omega \int \int \Delta\kappa(\mathbf{r}_1, \omega) \delta(\mathbf{r}_1 - \mathbf{r}_2) \\ &\times |R(\omega)|^2 G(\mathbf{r}_1, \mathbf{r}_A) G_0^*(\mathbf{r}_2, \mathbf{r}_B) dV_1 dV_2 = \\ &-i\omega \left\langle \int G(\mathbf{r}_1, \mathbf{r}_A) q(\mathbf{r}_1) dV_1 \right. \\ &\times \left. \left(\int G_0(\mathbf{r}_2, \mathbf{r}_B) q(\mathbf{r}_2) dV_2 \right)^* \right\rangle. \end{aligned} \tag{38}$$

Using the definitions in Eq. (37), Eq. (38) yields

$$G_S(\mathbf{r}_B, \mathbf{r}_A) = \frac{-i\omega}{|R(\omega)|^2} \langle p(\mathbf{r}_A) p_0^*(\mathbf{r}_B) \rangle. \tag{39}$$

This equation shows that the perturbation response between $\mathbf{r}_B$ and $\mathbf{r}_A$ can be extracted simply by cross correlating the perturbed pressure field observed at $\mathbf{r}_A$ with the unperturbed pressure measured at $\mathbf{r}_B$. This cross correlation must be compensated for the spectrum $|R(\omega)|^2$ and multiplied by $i\omega$ (i.e., differentiated with respect to time).

Equation (39) is useful in understanding the energy partitioning requirements for the reconstruction of the desired scattered-wave response. Let us consider, for example, Eq. (39) for the configuration of case I [Fig. 2, Eq. (17)]. In that case, according to Eq. (37), the volume sources that are locally proportional to the medium perturbation are restricted to $\mathbb{P}$. This results in a nonzero net flux that is outgoing energy at the boundary of $\mathbb{P}$ [we illustrate this in Fig. 6(a)]. As a consequence, there are also preferred directions of energy flux at the observation points $\mathbf{r}_{A,B}$. This situation is completely different than the condition of *equipartitioning* required for the reconstruction of either G_0 or G [7,25], which requires that the total energy flux within any direction at the receivers be equal to zero. To describe scattering, the flux at the sensor acts as a source must be so that it radiates energy only toward the position of the scatterers. If the scatterers are spatially restricted and located away from a sensor, then

when acting as pseudosource this sensor only needs a limited radiation aperture to fully reconstruct the scattered field. This explains why in the examples of case I [e.g., Eqs. (21), (30), and (32)] the full scattered field is retrieved with a finite source aperture as long as the sensor acting as a source lies between the physical sources and the scatterers.

VI. SCATTERING IN ATTENUATIVE MEDIA

To incorporate energy losses in wave propagation and scattering, we take $\kappa_0(\mathbf{r}), \kappa(\mathbf{r}) \in \mathbb{C}$ [e.g., in Eq. (1)] [30]. By using this in Eq. (8), Eq. (9) becomes

$$\oint_{\mathbf{r} \in \partial \mathbb{V}} [p_S^A \mathbf{v}_0^{B*} + p_0^{B*} \mathbf{v}_S^A] \cdot d\mathbf{S} = \int_{\mathbf{r} \in \mathbb{V}} p_S^A q_0^{B*} dV$$
$$+ \int_{\mathbf{r} \in \mathbb{V}} i\omega(\kappa_0^* - \kappa) p^A p_0^{B*} dV,$$
(40)

where now we have κ_0^* instead of simply κ_0 [Eq. (9)]. Then, using Green's functions [Eqs. (10) and (11)] and defining the complex scattering potential as $\mathcal{V}(\mathbf{r}) = \omega^2 \rho [\mathrm{Re}(\kappa - \kappa_0)$

$+i \, \mathrm{Im}(\kappa - \kappa_0)]$ (where Re and Im denote real and imaginary components, respectively), we obtain

$$G_S(\mathbf{r}_A, \mathbf{r}_B) = \oint_{\mathbf{r} \in \partial \mathbb{V}} \frac{1}{i\omega\rho} [G_0^*(\mathbf{r}_B, \mathbf{r}) \, \boldsymbol{\nabla} \, G_S(\mathbf{r}_A, \mathbf{r})$$
$$- G_S(\mathbf{r}_A, \mathbf{r}) \, \boldsymbol{\nabla} \, G_0^*(\mathbf{r}_B, \mathbf{r})] \cdot d\mathbf{S}$$
$$+ \int_{\mathbf{r} \in \mathbb{V}} \frac{1}{i\omega\rho} G(\mathbf{r}_A, \mathbf{r}) \mathrm{Re}\{\mathcal{V}(\mathbf{r})\} G_0^*(\mathbf{r}_B, \mathbf{r}) dV$$
$$+ \int_{\mathbf{r} \in \mathbb{V}} \frac{1}{\omega\rho} G(\mathbf{r}_A, \mathbf{r}) \mathrm{Im}\{\mathcal{V}(\mathbf{r})\} G_0^*(\mathbf{r}_B, \mathbf{r}) dV$$
$$- \int_{\mathbf{r} \in \mathbb{V}} 2\omega \, \mathrm{Im}\{\kappa_0\} G(\mathbf{r}_A, \mathbf{r}) G_0^*(\mathbf{r}_B, \mathbf{r}) dV. \quad (41)$$

The first volume integral in Eq. (41) yields the volume integral in Eq. (14), while the other volume integral accounts for scattering attenuation. Note that in attenuative media, even if there is no perturbation (i.e., $\mathcal{V}=0$), the last volume integral in Eq. (41) is nonzero. This case is analyzed by Snieder [30].

Let us revisit case I [Fig. 2 and Eq. (17)], but now consider it in attenuative media, i.e.,

(i) $\mathrm{Re}\{\mathcal{V}(\mathbf{r})\} \neq 0 \ \mathrm{Im}\{\mathcal{V}(\mathbf{r})\} \neq 0$; only for $\mathbf{r} \in \mathbb{P}; \ \mathbb{P} \subset \mathbb{R}^d$

(ii) sing supp$[\mathrm{Re}\{\mathcal{V}(\mathbf{r})\}] \neq 0$; (i.e., $\mathcal{V}$ generates backscattering)

(iii) $\mathbf{r}_B \notin \mathbb{P}$; (i.e., perturbations away from receiver acting as source)

(iv) $\kappa_0(\mathbf{r}), \ \rho_0(\mathbf{r}) \in C^\infty(\mathbb{R}^d)$; (i.e., smooth background)

(v) $[iG_0(\mathbf{r}, \mathbf{r}_s)]^{-1} \, \boldsymbol{\nabla} \, G_0(\mathbf{r}, \mathbf{r}_s) \cdot \mathbf{n}(\mathbf{r}_s) > 0$; for $(\mathbf{r}, \mathbf{r}_s) \in \partial \mathbb{V}_b$ or $\partial \mathbb{V}_t$ (i.e., outgoing reference waves)

$[iG_S(\mathbf{r}, \mathbf{r}_s)]^{-1} \, \boldsymbol{\nabla} \, G_S(\mathbf{r}, \mathbf{r}_s) \cdot \mathbf{n}(\mathbf{r}_s) < 0$; for $(\mathbf{r}, \mathbf{r}_s) \in \partial \mathbb{V}_b$ (i.e., ingoing scattered waves)

(vi) $\mathrm{Im}\{\kappa_0(\mathbf{r})\} = 0, \quad \forall \, \mathbf{r} \in \mathbb{R}^d$; or, (i.e., background is lossless)

(vi$'$) $\mathrm{Im}\{\kappa_0(\mathbf{r})\} \neq 0$; only for $\mathbf{r} \in \mathbb{P}$; (i.e., background attenuation is restricted to $\mathbb{P}$)

(42)

Next, under the same arguments as those used to derive Eqs. (19)–(21), it immediately follows that, for $\mathbb{P} \not\subset \mathbb{V}$ [Fig. 2(c)],

$$0 = \int_{\mathbf{r} \in \mathbb{V}} \frac{1}{i\omega\rho} G(\mathbf{r}_A, \mathbf{r}) \mathrm{Re}\{\mathcal{V}(\mathbf{r})\} G_0^*(\mathbf{r}_B, \mathbf{r}) dV$$
$$+ \int_{\mathbf{r} \in \mathbb{V}} \frac{1}{\omega\rho} G(\mathbf{r}_A, \mathbf{r}) \mathrm{Im}\{\mathcal{V}(\mathbf{r})\} G_0^*(\mathbf{r}_B, \mathbf{r}) dV$$
$$- \int_{\mathbf{r} \in \mathbb{V}} 2\omega \, \mathrm{Im}\{\kappa_0\} G(\mathbf{r}_A, \mathbf{r}) G_0^*(\mathbf{r}_B, \mathbf{r}) dV \quad (43)$$

and that therefore Eqs. (20) and (21) are also valid for scattered waves in attenuative media. By extension to when $\mathbb{P} \subset \mathbb{V}$ in case I [Fig. 2(b)], it is also true that

$$\int_{\mathbf{r} \in \partial \mathbb{V}_b} \frac{1}{i\omega\rho} [G_0^*(\mathbf{r}_B, \mathbf{r}) \, \boldsymbol{\nabla} \, G_S(\mathbf{r}_A, \mathbf{r}) - G_S(\mathbf{r}_A, \mathbf{r}) \, \boldsymbol{\nabla} \, G_0^*(\mathbf{r}_B, \mathbf{r})] \cdot d\mathbf{S}$$

$$= \int_{\mathbf{r} \in \mathbb{V}} \frac{1}{i\omega\rho} G(\mathbf{r}_A, \mathbf{r}) \mathrm{Re}\{\mathcal{V}(\mathbf{r})\} G_0^*(\mathbf{r}_B, \mathbf{r}) dV$$

$$+ \int_{\mathbf{r} \in \mathbb{V}} \frac{1}{\omega\rho} G(\mathbf{r}_A, \mathbf{r}) \mathrm{Im}\{\mathcal{V}(\mathbf{r})\} G_0^*(\mathbf{r}_B, \mathbf{r}) dV$$

$$- \int_{\mathbf{r} \in \mathbb{V}} 2\omega \, \mathrm{Im}\{\kappa_0\} G(\mathbf{r}_A, \mathbf{r}) G_0^*(\mathbf{r}_B, \mathbf{r}) dV. \quad (44)$$

Thus the general result of Eq. (21), discussed in Sec. V, is also valid for attenuative scattered waves regardless of the choice of configurations for $\partial \mathbb{V}_b$ or $\mathbf{r}_A$ (Fig. 2). So just as in lossless media, it is possible to retrieve the full scattered response generated by soft and/or attenuative targets by cross

correlation of scattered and reference waves over a limited source aperture.

To understand why the result above holds for attenuative media, consider applying homogeneous Dirichlet or Neumann conditions on $\partial\mathbb{V}$ in Eq. (41), which yields

$$G_S(\mathbf{r}_A,\mathbf{r}_B) = \int_{\mathbf{r}\in\mathbb{V}} \frac{1}{i\omega\rho} G(\mathbf{r}_A,\mathbf{r}) \mathrm{Re}\{\mathcal{V}(\mathbf{r})\} G_0^*(\mathbf{r}_B,\mathbf{r}) dV$$

$$+ \int_{\mathbf{r}\in\mathbb{V}} \frac{1}{\omega\rho} G(\mathbf{r}_A,\mathbf{r}) \mathrm{Im}\{\mathcal{V}(\mathbf{r})\} G_0^*(\mathbf{r}_B,\mathbf{r}) dV$$

$$- \int_{\mathbf{r}\in\mathbb{V}} 2\omega\,\mathrm{Im}\{\kappa_0\} G(\mathbf{r}_A,\mathbf{r}) G_0^*(\mathbf{r}_B,\mathbf{r}) dV. \quad (45)$$

We now consider random volume sources similar to Eq. (37) but now described by

$$\langle q(\mathbf{r}_1,\omega)q^*(\mathbf{r}_2,\omega)\rangle = \mathcal{Q}(\mathbf{r}_1)\delta(\mathbf{r}_1-\mathbf{r}_2)|R(\omega)|^2. \quad (46)$$

Note that at every point in the volume, the quantity $\mathcal{Q}(\mathbf{r}) = \Delta\kappa'(\mathbf{r}) = \kappa_0^*(\mathbf{r}) - \kappa(\mathbf{r})$ in Eq. (46) describes sources which are locally proportional to (i) $\mathrm{Re}\{\mathcal{V}\}$, (ii) $\mathrm{Im}\{\mathcal{V}\}$, and (iii) $\mathrm{Im}\{\kappa_0\}$, respectively. Through a derivation analogous to Eq. (38), Eq. (45) gives

$$G_S(\mathbf{r}_B,\mathbf{r}_A) = \frac{-i\omega}{|R(\omega)|^2}\langle p(\mathbf{r}_A)p_0^*(\mathbf{r}_B)\rangle, \quad (47)$$

same as in Eq. (39). For the conditions defining case I in attenuative media [Eq. (42)], the result in Eq. (47) implies a flux of outgoing energy at the boundary of $\mathbb{P}$, same as in the lossless case [Fig. 6(a)]. As with lossless scattering, the receiver that acts as a pseudosource needs only a limited radiation aperture to retrieve the full attenuative scattered-wave response for case I; this is why the limited source aperture used in Eq. (21) also accounts for attenuative scattering. This scenario is no longer true, however, if the background is attenuative, i.e., if conditions (vi) or (vi′) in Eq. (42) do not hold. In that case, the result in Eq. (47) requires the ignition of volume sources everywhere that are locally proportional to the background loss parameters. This leads to an interchange of energy through the boundary of $\mathbb{P}$, as depicted in Fig. 6(b). This in turn implies that, although energy equipartitioning is still not a necessary requirement, the correct pseudoresponse between receivers cannot be retrieved with a limited radiation aperture; consequently, Eq. (21) would no longer hold.

VII. APPLICATION EXAMPLE: OCEAN-BOTTOM SEISMICS

Here we discuss the application of scattering reciprocity to seismic data acquired on the ocean bottom. A general concept of ocean-bottom seismic data acquisition is shown in Fig. 7. There, active physical sources are placed on $\partial\mathbb{V}_t$ and sensors are positioned on the seafloor. The objective of ocean-bottom seismic experiments is to characterize the scattering potential in the subsurface (i.e., in $\mathbb{P}$; Fig. 7) from the recorded scattered waves. Since the surface of the ocean acts as a perfectly reflecting boundary for acoustic waves that
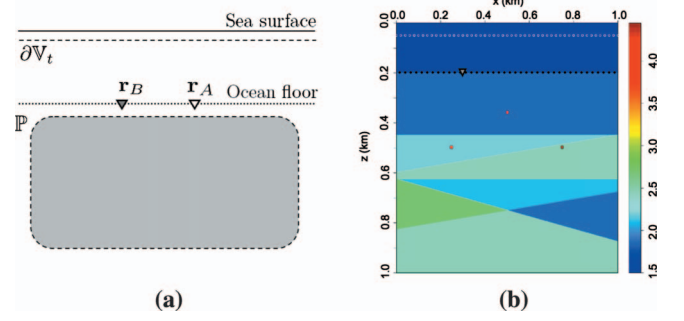

FIG. 7. (Color) Application of scattering reciprocity to acoustic waves recorded on the ocean bottom. The cartoon in (a) relates the specific case of ocean-floor seismology with the configuration of case I (Fig. 2). Panel (b) shows the perturbed acoustic wave speed model used in the numerical experiment. In the model, the solid dotted line at 0.2 km depth represents the instrumented ocean bottom, the open dotted line depicts the positions of physical sources, and the triangle represents the location of the pseudosource in the numerical examples. Note that, in the model in (b), the perturbations in $\mathbb{P}$ consist of the scatterers and interfaces located below the depth of 0.3 km. The color bar portrays model wave speeds in km/s.

propagate in the experiment in Fig. 7, the recorded data contain not only the desired subsurface scattered waves but also the reverberations that occur between the ocean surface, the sea bottom, and subsurface scatterers. These reverberations become a strong source of coherent noise in extracting information about the Earth's interior. Here we show that the scattering-based reciprocity relations developed in this paper can be used to remove the effect of surface-related reverberations from ocean-bottom seismic data, thus facilitating the retrieval of information associated only with subsurface scattered waves.

Scattered waves described by reciprocity relations such as in Eq. (18) satisfy boundary and initial conditions imposed on $\partial\mathbb{V}$ (or in case I in $\partial\mathbb{V}_b\cup\partial\mathbb{V}_t$), but it can be used to relate different wave states that have varying material properties and/or boundary conditions *outside* of $\mathbb{V}$ [2,3]. In the particular case of ocean-bottom seismics, the reciprocity relation in Eq. (18) can relate scattered waves in the presence of the ocean's free surface[2] with waves without the free surface. Note that the result in Eq. (21) is approximate for the case in Fig. 7 because it violates condition (v): this leads to the incomplete cancellation of terms necessary for Eq. (20) to hold. Furthermore, dipole acoustic sources are typically not available in ocean-bottom seismic experiments. However, many such experiments do measure dual fields, i.e., pressure and particle velocity, at the sea bottom. Since in the given experiment the source surface is flat and horizontal, i.e., $\mathbf{n} = \{0,0,n_3\}$ $\forall\mathbf{r}\in\partial\mathbb{V}_t$, then $\mathbf{v}(\mathbf{r},\mathbf{r}_{B,A})\cdot d\mathbf{S} = v_{i=3}(\mathbf{r},\mathbf{r}_{B,A})dS$. In the absence of vertically oriented dipole sources on $\partial\mathbb{V}_t$, we replace them by $v_{i=3}^{\mathrm{obs}}$ which is the response of monopole sources observed in the vertical component of the particle velocity field at the ocean bottom. This gives, after Eq. (21),

---

[2]The term "free-surface" indicates that homogeneous Dirichlet conditions apply on the ocean surface.
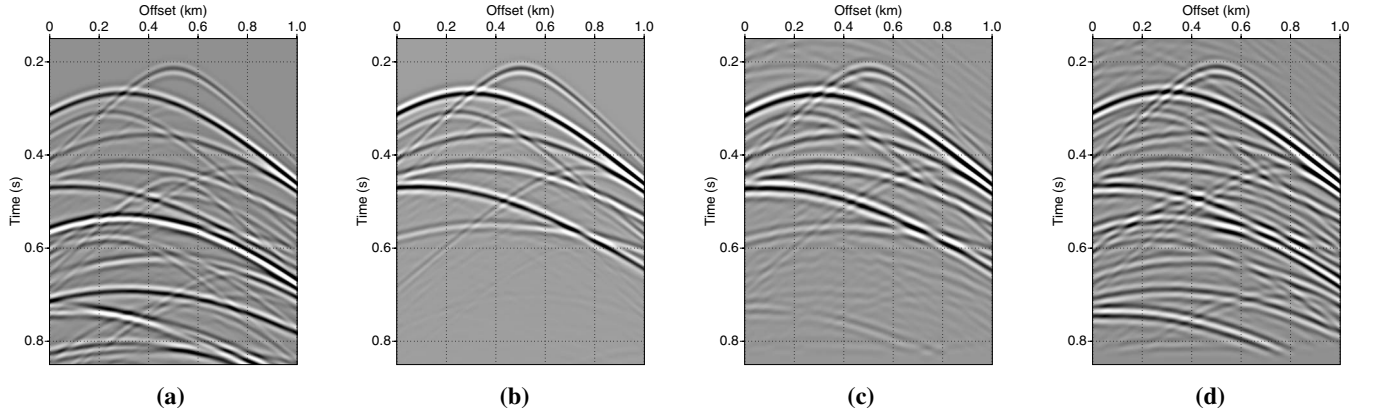
FIG. 8. Comparisons of true scattered-wave responses with pseudosource responses obtained by cross-correlating reference and scattered waves. The true scattered-wave responses for a physical source at (0.3 km, 0.2 km) [see Fig. 7(b)] are displayed in (a) modeled *with* a free surface (at $z=0$ km) and in (b) where it is modeled *without* a free surface. The responses in (c) and in (d) correspond to pseudosources retrieved via cross correlations. The result in (c) is obtained with Eq. (48), while (d) results from applying Eq. (49). It is important to note that the input data *to both* (c) and (d) were modeled *with* a free surface.

$$G_S(\mathbf{r}_A, \mathbf{r}_B) \approx \int_{\mathbf{r} \in \partial \mathbb{V}_t} \mathcal{F}(\omega)[p_S(\mathbf{r}_A, \mathbf{r})v_{3,0}^{\mathrm{obs}*}(\mathbf{r}_B, \mathbf{r})$$
$$+ p_0^*(\mathbf{r}_B, \mathbf{r})v_{3,S}^{\mathrm{obs}}(\mathbf{r}_A, \mathbf{r})]dS, \qquad (48)$$

where $\mathcal{F}(\omega)$ is a signal-shaping filter that accounts for the imprint of the source-time excitation function. Dipole sources on $\partial \mathbb{V}_t$ can only be exactly replaced by observed particle velocities on the seafloor if the surrounding medium was homogeneous. Therefore, using the observed quantities v_3^{obs} in Eq. (48) introduces errors in retrieving $G_S(\mathbf{r}_A, \mathbf{r}_B)$. Because the material heterogeneity in our experiment is associated with the scattering potential in $\mathbb{P}$ (Fig. 7), the errors introduced by replacing dipole sources with v_3^{obs} are of higher order in the scattered waves (i.e., they will be relatively weak in amplitudes). Most previous applications of retrieving inter-receiver Green's functions from seismic data rely on the cross correlations of pressure fields only, i.e.,

$$G_S(\mathbf{r}_A, \mathbf{r}_B) \approx \int_{\mathbf{r} \in \partial \mathbb{V}_t} \frac{2}{\rho c} \mathcal{F}(\omega)p_S(\mathbf{r}_A, \mathbf{r})p_0^*(\mathbf{r}_B, \mathbf{r})dS, \quad (49)$$

which assumes a far-field or Sommerfeld radiation boundary condition, e.g., [6]. In the example we present here we show and discuss the differences of using Eqs. (48) and (49) for the extraction of the multiple-free scattered-wave response between ocean-bottom seismometers.

The two-dimensional numerical simulation is done on the model shown in Fig. 7(b). This model represents the perturbed medium; the unperturbed medium consists only of the 0.2-km-deep water layer and a homogeneous half-space with a constant wave speed of 1800 m/s. The medium perturbation thus consists of all scatterers and interfaces lying deeper than 0.3 km [Fig. 7(b)]. Density is kept constant at 10^3 kg/m^3. We model the data using a finite-difference solution to the acoustic wave equation [e.g., Eq. (1)]. In the numerical experiment, pressure (i.e., monopole) sources are placed on a 0.01-km-deep horizontal line with a constant lateral spacing of 4 m; pressure and particle velocity fields

are measured by a line of sensors on the water bottom [i.e., at $z=0.2$ km; Fig. 7(b)] positioned at every 2 m. With this experiment configuration, we model the acoustic responses in both the reference and perturbed models. All of the data used in for retrieving the scattered-wave Green's functions between ocean-bottom sensors are modeled with free-surface (i.e., Dirichlet) boundary conditions on the top of the model.

In Figs. 8(c) and 8(d) we show the result of extracting the scattered-wave response between receivers using Eqs. (48) and (49), respectively. In both figures, the panels represent the responses recorded at all receivers (i.e., for varying $\mathbf{r}_A$), excited by a pseudosource synthesized in fixed receiver at $\mathbf{r}_B = (0.3 \text{ km}, 0.2 \text{ km})$ [triangle in Fig. 7(b)]. While Figs. 8(c) and 8(d) clearly show that the responses obtained via Eqs. (48) and (49) are different, it is important to note that the input field quantities used for evaluating the integrands satisfy the same boundary conditions. On the other hand, the responses of actual sources placed at (0.3 km, 0.2 km) depicted in Figs. 8(a) and 8(b) satisfy different boundary conditions: the pressure field in Fig. 8(a) satisfies $G_{0,S}(\mathbf{r})=0$ at the sea surface [i.e., free-surface conditions; same as the input fields for Figs. 8(c) and 8(d)], while for the response in Fig. 8(b) $G_{0,S}(\mathbf{r}) \neq 0$ on the ocean surface. The response obtained by Eq. (48) [Fig. 8(c)] approximates that of Fig. 8(b), whereas the response generated with Eq. (49) [Fig. 8(d)] is close to that of Fig. 8(a). In replacing the dipole sources required by Eq. (21) by the vertical component of particle velocity in Eq. (48), we achieve an effective cancellation between in- and out-going waves at $\partial \mathbb{V}_t$ that results in approximating the scattered-wave response without the free-surface condition present in the original experiment. On the other hand, by cross correlating only pressure scattered and reference waves [Eq. (49)], we assume that there are only out-going waves at $\partial \mathbb{V}_t$ and thus in- and out-going terms do not cancel. Consequently, when using Eq. (49) we retrieve scattered waves that approximate the true perturbations in the presence of free-surface boundary conditions [compare Figs. 8(a) and 8(d)].

With this numerical example we demonstrate that our formulations of scattering-based reciprocity can be used to ex-

tract scattered waves between receivers in ocean-bottom seismic experiments. Moreover, we show that by using different combinations of single- or dual-field measurements we extract scattered fields that satisfy different boundary conditions. This is a particularly important step in isolating or separating the reverberations caused by the water surface from ocean-bottom seismic data.

VIII. DISCUSSION AND CONCLUSION

In this paper, we present a suite of integral reciprocity equations for acoustic scattering that can be useful both for theoretical considerations and for applications in retrieving scattered waves via correlations and possibly in imaging or inversion of scattered fields.

A fundamental result in this paper is that the retrieval of scattered waves by cross correlations or cross convolutions does not necessarily rely on a closed surface integral or on invoking energy equipartitioning. This is an important difference between the work we present here and previous work in the field of Green's function retrieval from diffuse-wave correlation [9,17,31] or from correlation of deterministic wave fields [6,25], which do require energy equipartitioning. Most previous studies show that equipartitioning of energy is necessary to recover the superposition of the causal and anticausal wave fields G or G_0 (i.e., unperturbed or perturbed). Since for scattered fields equipartitioning is not a necessary requirement, our expressions isolate the wave field perturbations G_S separately from its anticausal counterpart G_S^*. Moreover, for systems that are invariant under time reversal, Green's function retrieval by wave field cross correlations requires only a surface integration [6,25,31], whereas the retrieval of the perturbations G_S from correlations of wave field perturbations with unperturbed wave fields requires additional volume integrals. Our analysis shows that, in fact, these volume terms *counteract* the contributions of closed surface terms, which reaffirms that, for arbitrarily spatially varying scattering potentials, the retrieval of scattered fields relies on uneven energy partitioning.

This requirement of uneven radiation for the retrieval of scattered waves can be advantageous for certain experiment configurations. In the case of scattered waves generated by remote perturbations, we demonstrate that the scattered field propagating between receivers is fully retrieved by correlating scattered and reference waves generated by sources in an open surface. Again, previous general formulations of Green's function retrieval [7,24,25] state that sources must surround the receivers to correctly retrieve, via cross correlations, the waves that propagate between receivers. In the absence of a closed source aperture, the retrieved responses are prone to dynamic distortions and artifacts [26,29]. This becomes a limitation for the retrieval of receiver responses by correlations in experiments where surrounding the medium with sources is not practical. If, however, the retrieval of scattered waves is the objective, then our results show that the scattered field can be accurately retrieved with a limited source array (for the configuration in Fig. 2). This is an important experimental advantage brought by the analysis of scattering-based reciprocity. Furthermore, it is important to note that these results hold both for lossless and attenuative scattering.

In this paper we present a direct application of scattering reciprocity to ocean-bottom seismic data, where we retrieve subsurface scattered waves from ocean-bottom receivers without the interference of reverberations generated by the water surface. Other applications of the scattering reciprocity relations to retrieving scattered signals have been proposed in [29,32,33]. In the context of retrieving scattered waves by cross correlation, the theory we discuss also draws experimental validation from the work of other authors. In particular, we point out the studies performed by Bakulin and Calvert [16] and by Mehta *et al.* [34], with their so-called *virtual source* method. Their methods explicitly correlate transmission and reflection responses to extract desired scattered waves and directly verify our results. Note that although most of the examples cited here come from the field of geophysics, our results are immediately applicable to other fields in acoustics such as physical oceanography, laboratory, and medical ultrasonics, and nondestructive testing.

While the derivations and examples presented here heavily focus on the application of scattering-based reciprocity to retrieving scattered responses by cross correlations, we point out some possible applications to inverse problems. One such application is the use for the exact form of the correlation-type representation theorems for the calculation of *Fréchet derivatives* [35], which consist of the partial derivatives of the wave field perturbations with respect to the medium perturbations. These derivatives can be directly derived from the theorems we provide here. These derivatives are important for the computation of sensitivity kernels used in wave form inversion [35,36], in imaging [37], or in formulations of wave-equation based tomography [36,38]. Still in the context of inverse scattering [5,37], the theory we present here is used in [39] for establishing formal connections between different approaches in imaging such as seismic migration [40,41], time-reversal methods [42,43], and image-domain inverse scattering [41,44].

Apart from imaging applications, our results (both in terms of retrieving wave field perturbations and for estimating medium perturbations) can be used for monitoring temporal changes in the medium. In geoscience, this could be applied to remotely monitoring the depletion of aquifers or hydrocarbon reservoirs or monitoring the injection of CO_2 for carbon sequestration. In materials science, our results can be used to monitor material integrity with respect, for example, to temporal changes in temperature or changes due to crack formation. The detection of earthquake damage is a potential application in the field of structural engineering. Within medical imaging applications, our expressions can be tailored, for instance, to observe the evolution of living tissue (e.g., transplants and tumors) from a series of time-lapse ultrasonic measurements.
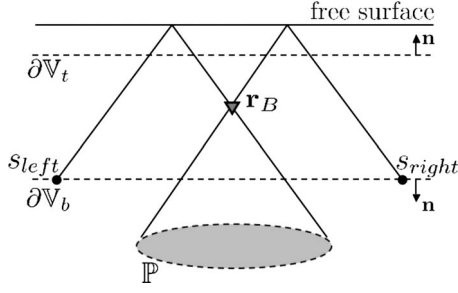
FIG. 9. Illustration of stationary points on the bottom surface $\partial \mathbb{V}_b$ that yield physical contributions to scattered waves that propagate between the observation points.
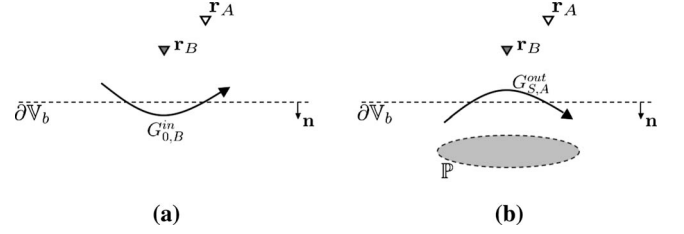

FIG. 10. Cartoons representing the conditions required for the bottom-surface integral to vanish in the case of Eq. (20). Panel (a) states that ingoing reference waves due to sources on $\partial \mathbb{V}_b$ must be absent, whereas (b) indicates that there should be no outgoing scattered waves excited by sources on $\partial \mathbb{V}_b$.

APPENDIX A: CONDITIONS FOR A VANISHING INTEGRAL OVER $\partial \mathbb{V}_b$

To determine the situation when the surface integral for the bottom surface in Eq. (20) vanishes, we first observe that in general this surface integral cannot vanish. For example, consider the case when there is a free surface present above the bottom surface $\partial \mathbb{V}_b$ (Fig. 9). Then there will be stationary sources on the bottom surface that contribute to the construction of the scattered field with a source at location $\mathbf{r}_B$. The drawn propagation paths in Fig. 9 are the outermost paths that are still needed to illuminate the scattering region with sources on the surface $\partial \mathbb{V}_b$, and indeed all the sources in between s_{left} and s_{right} on the integration surface give stationary contributions to the surface integral.

To see in which special cases the surface integral does vanish, we follow [6] and decompose the wave field into in-going and out-going waves of the volume $\mathbb{V}$. That is, we assume

$$G_0 = G_0^{in} + G_0^{out}, \tag{A1}$$

$$G_S = G_S^{in} + G_S^{out}. \tag{A2}$$

Using this in Eq. (20), it follows that

$$\int_{\partial \mathbb{V}_b} \frac{1}{i\omega\rho} \{ G_{0,B}^* \boldsymbol{\nabla} G_{S,A} - G_{S,A} \boldsymbol{\nabla} G_{0,B}^* \} \cdot d\mathbf{S}$$

$$= \int_{\partial \mathbb{V}_b} \frac{1}{i\omega\rho} \{ (G_{0,B}^{in*} + G_{0,B}^{out*})(\boldsymbol{\nabla} G_{S,A}^{in} + \boldsymbol{\nabla} G_{S,A}^{out}) - (G_{S,A}^{in} + G_{S,A}^{out})$$

$$\times (\boldsymbol{\nabla} G_{0,B}^{in*} + \boldsymbol{\nabla} G_{0,B}^{out*}) \} \cdot d\mathbf{S}, \tag{A3}$$

where we introduced the shorthand notation $G_{(S,0),(A,B)} = G_{(S,0)}(\mathbf{r}_{A,B}, \mathbf{r})$ with the subscripts $(S,0)$ indicating either the scattered (S) or background (0) Green's function, while the subscripts (A,B) denote the receiver location at either $\mathbf{r}_A$ (A) or $\mathbf{r}_B$ (B). Following again [6] and assuming that the medium is locally smooth around $\partial \mathbb{V}_b$, we can approximate the gradients by a multiplication of the Green's function with

$\pm i |\cos \alpha(\mathbf{x})| \omega / c(\mathbf{x})$, where $c(\mathbf{x})$ is the local velocity at $\partial \mathbb{V}_b$ and $\alpha(\mathbf{x})$ is the local angle between the ray and the normal on $\partial \mathbb{V}_b$. The minus sign relates to waves traveling into $\mathbb{V}$, while the plus sign relates to waves traveling out of $\mathbb{V}$. By the exact same reasoning as [6] it follows that at the stationary source locations on $\partial \mathbb{V}_b$ the absolute values of the cosines of the ray angles are the same for $G_{S,A}$ and $G_{0,B}$. That means that contributions of the terms in Eq. (A3) with products of in- and out-going Green's functions give exactly opposite contributions. Therefore these "cross" terms do not contribute to the surface integral, leaving the surface integral as

$$\int_{\partial \mathbb{V}_b} \frac{1}{i\omega\rho} \{ G_{0,B}^* \boldsymbol{\nabla} G_{S,A} - G_{S,A} \boldsymbol{\nabla} G_{0,B}^* \} \cdot d\mathbf{S}$$

$$= \int_{\partial \mathbb{V}_b} \frac{2}{i\omega\rho} \{ G_{S,A}^{in} \boldsymbol{\nabla} G_{0,B}^{in*} + G_{S,A}^{out} \boldsymbol{\nabla} G_{0,B}^{out*} \} \cdot d\mathbf{S}. \tag{A4}$$

From Eq. (A4) it is easy to see when the surface integral vanishes. The only meaningful situations to consider are the cases

   (i) $G_{S,A}^{in} = 0$ and $\hat{\mathbf{n}} \cdot \boldsymbol{\nabla} G_{0,B}^{out} = 0$ and

   (ii) $G_{S,A}^{out} = 0$ and $\hat{\mathbf{n}} \cdot \boldsymbol{\nabla} G_{0,B}^{in} = 0$,

where $\hat{\mathbf{n}}$ is the outward pointing normal on $\partial \mathbb{V}_b$. We are interested in analyzing when the surface integral vanishes if the surface $\partial \mathbb{V}_b$ is above the perturbation volume $\mathbb{P}$. In this situation case (i) is not really relevant, as then there would be no energy scattering into the volume $\mathbb{V}$, which is not a common situation encountered. Therefore case (ii) provides the relevant conditions when the surface integral vanishes. This means that there cannot be any scattered energy traveling outward of $\mathbb{V}$ through $\partial \mathbb{V}_b$. That is, scattered energy is not allowed to change propagation direction from into $\mathbb{V}$ to out of $\mathbb{V}$ above $\partial \mathbb{V}_b$ (or from up to down in case $\partial \mathbb{V}_b$ is horizontal). Moreover, the background wave field cannot change propagation direction from out of $\mathbb{V}$ to into $\mathbb{V}$ below $\partial \mathbb{V}_b$ (or from down to up in case $\partial \mathbb{V}_b$ is horizontal). Both these conditions are summarized in Fig. 10.

APPENDIX B: ANALYSIS OF THE SCATTERED-WAVE RESPONSES FOR THE ONE-LAYER MODEL

In this appendix we derive Green's function extraction for the 1D model of Fig. 5. Within every layer, the solution

consists of the superposition of waves $\exp(\pm ikz)$, with k as the wave number in each layer. Since $\frac{d\rho(z)}{dz}=0$, $G(z,z_0)$ $\in C^2(\mathbb{R}^1)$. For a source above the layer ($z_0 < 0$) this leads to the following exact Green's function for $z < 0$:

$$G(z,z_0) = \frac{\rho c_0}{2}e^{ik_0|z-z_0|} + \frac{\rho c_0}{2}\frac{i}{2D}\left(\frac{k_1}{k_0}-\frac{k_0}{k_1}\right)\sin k_1 H e^{-ik_0(z+z_0)},$$

(B1)

while for $0 < z < H$

$$G(z,z_0) = \frac{\rho c_0}{2}\frac{1}{2D}\left(1+\frac{k_0}{k_1}\right)e^{ik_1(z-H)-ik_0z_0}$$
$$+ \frac{\rho c_0}{2}\frac{1}{2D}\left(1-\frac{k_0}{k_1}\right)e^{-ik_1(z-H)-ik_0z_0}$$

(B2)

and for $z > H$

$$G(z,z_0) = \frac{\rho c_0}{2}\frac{1}{D}e^{ik_0(z-H-z_0)},$$

(B3)

with

$$D = \cos k_1 H - \frac{i}{2}\left(\frac{k_1}{k_0}+\frac{k_0}{k_1}\right)\sin k_1 H.$$

(B4)

For $z < 0$ the perturbed field is given by the last term of expression (B1), while for $z > H$ the perturbed field $G_S = G - G_0$ follows by subtracting expressions (B3) and (25),

$$G_S(z,z_0) = \frac{\rho c_0}{2}\frac{1}{D}e^{ik_0(z-z_0)}(e^{-ik_0H}-D).$$

(B5)

We first compute the contribution S_- when both receivers are above the layer [panel (a) of Fig. 5]. Inserting the last term of expression (B1) and Eq. (25) into expression (27) gives

$$S_-(z_B,z_A) = \frac{2}{\rho c_0}\frac{\rho c_0}{2}\frac{i}{2D}\left(\frac{k_1}{k_0}-\frac{k_0}{k_1}\right)$$
$$\times\sin k_1 H e^{-ik_0(z_A+z_-)}\frac{\rho c_0}{2}e^{-ik_0(z_B-z_-)}$$
$$= \frac{\rho c_0}{2}\frac{i}{2D}\left(\frac{k_1}{k_0}-\frac{k_0}{k_1}\right)\sin k_1 H e^{-ik_0(z_A+z_B)}.$$

(B6)

A comparison with the last term of expression (B1) shows that S_- gives the perturbed Green's function [expression (30)]. The contribution from a source below the layer [panel (b) of Fig. 5] follows by inserting expressions (25) and (B5) into Eq. (28),

$$S_+(z_B,z_A) = \frac{2}{\rho c_0}\frac{\rho c_0}{2}\frac{e^{ik_0(z_+-z_A)}}{D}(e^{-ik_0H}-D)\frac{\rho c_0}{2}e^{-ik_0(z_+-z_B)}$$
$$= \frac{\rho c_0}{2}\frac{e^{ik_0(z_B-z_A)}}{D}(e^{-ik_0H}-D).$$

(B7)

To get the volume term [panel (c) of Fig. 5] we insert expressions (25) and (B2) into Eq. (29) to give

$$V(z_B,z_A) = \frac{i}{\rho\omega}(k_0^2-k_1^2)\frac{\rho c_0}{2}\frac{1}{2D}\times\int_0^H\left[\left(1+\frac{k_1}{k_0}\right)e^{ik_1(z-H)-ik_0z_A}\right.$$
$$\left.+\left(1-\frac{k_1}{k_0}\right)e^{-ik_1(z-H)-ik_0z_A}\right]\frac{\rho c_0}{2}e^{-ik_0(z-z_B)}dz.$$

(B8)

Carrying out the z integration and rearranging terms gives

$$V(z_B,z_A) = -\frac{\rho c_0}{2}\frac{1}{2D}e^{ik_0(z_B-z_A)}\left\{\left[1+\frac{1}{2}\left(\frac{k_0}{k_1}+\frac{k_1}{k_0}\right)\right]\right.$$
$$\times(e^{-ik_0H}-e^{-ik_1H})+\left[1-\frac{1}{2}\left(\frac{k_0}{k_1}+\frac{k_1}{k_0}\right)\right]$$
$$\left.\times(e^{-ik_0H}-e^{ik_1H})\right\}.$$

(B9)

The term between curly brackets satisfies

$$[\cdots] = 2e^{-ik_0H} - (e^{ik_1H}+e^{-ik_1H}) + \frac{1}{2}\left(\frac{k_0}{k_1}+\frac{k_1}{k_0}\right)(e^{ik_1H}-e^{-ik_1H})$$
$$= 2(e^{-ik_0H}-D),$$

(B10)

where expression (B4) is used in the last identity. Using this result gives

$$V(z_B,z_A) = -\frac{\rho c_0}{2}\frac{1}{D}(e^{-ik_0H}-D)e^{ik_0(z_B-z_A)}.$$

(B11)

A comparison with Eq. (B7) proves expression (31).

We next consider the situation where the receivers are on opposite sides of the layer [panels (d)–(f) in Fig. 5]. The term S_+ [panel (e)] follows by combining expressions (25), (28), and (B5) to give

$$S_+(z_B,z_A) = \frac{2}{\rho c_0}\frac{\rho c_0}{2}\frac{1}{D}e^{ik_0(z_+-z_A)}(e^{-ik_0H}-D)\frac{\rho c_0}{2}e^{-ik_0(z_+-z_B)}$$
$$= \frac{\rho c_0}{2}\frac{1}{D}e^{ik_0(z_B-z_A)}(e^{-ik_0H}-D).$$

(B12)

A comparison with expression (B5) shows that this equals the field perturbation [expression (32)]. The contribution from the other end point [panel (d) in Fig, 5] follows by combining expressions (25), (27), and (B1),

$$S_-(z_B,z_A) = \frac{2}{\rho c_0}\frac{\rho c_0}{2}\frac{i}{2D}\left(\frac{k_1}{k_0}-\frac{k_0}{k_1}\right)$$
$$\times\sin k_1 H e^{-ik_0(z_-+z_A)}\frac{\rho c_0}{2}e^{-ik_0(z_B-z_-)}$$
$$= \frac{\rho c_0}{2}\frac{i}{2D}\left(\frac{k_1}{k_0}-\frac{k_0}{k_1}\right)\sin k_1 H e^{-ik_0(z_A+z_B)}.$$

(B13)

The volume term [panel (f) of Fig. 5] follows from combining expressions (25), (29), and (B2),

$$V(z_B, z_A) = \frac{i}{\rho\omega}(k_0^2 - k_1^2)\frac{\rho c_0}{2}\frac{1}{2D} \times \int_0^H \left[\left(1 + \frac{k_0}{k_1}\right)e^{ik_1(z-H)-ik_0 z_A} \right.$$

$$\left. + \left(1 - \frac{k_0}{k_1}\right)e^{-ik_1(z-H)-ik_0 z_A} \right] \frac{\rho c_0}{2}e^{-ik_0(z_B-z)}dz. \quad \text{(B14)}$$

Carrying out the z integration and using that $\omega/k_0 = c_0$ give

$$V(z_B, z_A) = \frac{i}{\rho\omega}(k_0^2 - k_1^2)\left(\frac{\rho c_0}{2}\right)^2\frac{1}{2D}\frac{2}{k_1}\sin k_1 H e^{-ik_0(z_A+z_B)}$$

$$= -\frac{\rho c_0}{2}\frac{i}{2D}\left(\frac{k_1}{k_0} - \frac{k_0}{k_1}\right)\sin k_1 H e^{-ik_0(z_A+z_B)}. \quad \text{(B15)}$$

Together with Eq. (B13) this proves Eq. (33).

---

[1] J. W. S. Rayleigh, *The Theory of Sound* (Dover, New York, 1878) (reprint 1945).

[2] A. de Hoop, J. Acoust. Soc. Am. **84**, 1877 (1988).

[3] J. T. Fokkema and P. M. van den Berg, *Seismic Applications of Acoustic Reciprocity* (Elsevier, New York, 1993).

[4] A. J. Berkhout and D. J. Verschuur, Geophysics **62**, 1586 (1997).

[5] A. B. Weglein, F. V. Araújo, P. M. Carvalho, R. H. Stolt, K. H. Matson, R. T. Coates, D. Corrigan, D. J. Foster, S. A. Shaw, and H. Zhang, Inverse Probl. **19**, R27 (2003).

[6] K. Wapenaar and J. Fokkema, Geophysics **71**, SI133 (2006).

[7] K. Wapenaar, E. Slob, and R. Snieder, Phys. Rev. Lett. **97**, 234301 (2006).

[8] O. I. Lobkis and R. L. Weaver, J. Acoust. Soc. Am. **110**, 3011 (2001).

[9] R. L. Weaver and O. I. Lobkis, Phys. Rev. Lett. **87**, 134301 (2001).

[10] N. M. Shapiro, M. Campillo, L. Stehly, and M. H. Ritzwoller, Science **307**, 1615 (2005).

[11] R. Snieder, Phys. Rev. E **69**, 046610 (2004).

[12] J. F. Claerbout, Geophysics **33**, 264 (1968).

[13] K. Wapenaar, J. Thorbecke, and D. Draganov, Geophys. J. Int. **156**, 179 (2004).

[14] K. G. Sabra, P. Gerstoft, P. Roux, W. A. Kuperman, and M. Fehler, Geophys. Res. Lett. **32**, L14311 (2005).

[15] G. T. Schuster, F. Followill, L. J. Katz, J. Yu, and Z. Liu, Geophysics **68**, 1685 (2003).

[16] A. Bakulin and R. Calvert, Geophysics **71**, SI139 (2006).

[17] A. E. Malcolm, J. A. Scales, and B. A. van Tiggelen, Phys. Rev. E **70**, 015601(R) (2004).

[18] K. van Wijk, Geophysics **71**, SI79 (2006).

[19] J. E. Rickett and J. F. Claerbout, The Leading Edge **18**, 957 (1999).

[20] R. Snieder and E. Şafak, Bull. Seismol. Soc. Am. **96**, 586 (2006).

[21] D. Thompson and R. Snieder, The Leading Edge **25**, 1093 (2006).

[22] P. Roux, W. A. Kuperman, and NPAL Group, J. Acoust. Soc. Am. **116**, 1995 (2004).

[23] K. G. Sabra, P. Roux, A. M. Thode, G. L. D'Spain, and W. S. Hodgkiss, IEEE J. Ocean. Eng. **30**, 338 (2005).

[24] R. L. Weaver and O. I. Lobkis, J. Acoust. Soc. Am. **116**, 2731 (2004).

[25] R. Snieder, K. Wapenaar, and U. Wegler, Phys. Rev. E **75**, 036103 (2007).

[26] R. L. Weaver, Wave Motion **45**, 596 (2008).

[27] L. S. Rodberg and R. M. Thaler, *Introduction to the Quantum Theory of Scattering* (Academic Press, New York, 1967).

[28] R. Snieder, K. van Wijk, M. Haney, and R. Calvert, Phys. Rev. E **78**, 036606 (2008).

[29] I. Vasconcelos and R. Snieder, Geophysics **73**, S115 (2008).

[30] R. Snieder, J. Acoust. Soc. Am. **121**, 2637 (2007).

[31] E. Larose, L. Margerin, A. Derode, B. van Tiggelen, M. Campillo, N. Shapiro, A. Paul, L. Stehly, and M. Tanter, Geophysics **71**, SI11 (2006).

[32] I. Vasconcelos, R. Snieder, and B. Hornby, Geophysics **73**, S157 (2008).

[33] I. Vasconcelos, R. Snieder, S. T. Taylor, P. Sava, J. A. Chavarria, and P. Malin, EOS Trans. Am. Geophys. Union **89**, 349 (2008).

[34] K. Mehta, A. Bakulin, J. Sheiman, R. Calvert, and R. Snieder, Geophysics **72**, V79 (2007).

[35] A. Tarantola, *Inverse Problem Theory* (Elsevier, Amsterdam, 1987).

[36] J. Tromp, C. Tape, and Q. Liu, Geophys. J. Int. **160**, 195 (2005).

[37] D. Colton and R. Kress, *Inverse Acoustic and Electromagnetic Scattering Theory* (Springer-Verlag, Berlin, 1992).

[38] M. Woodward, Geophysics **57**, 15 (1992).

[39] I. Vasconcelos, SEG Exp. Abstr. **27**, 2927 (2008).

[40] J. F. Claerbout, *Imaging the Earth's Interior* (Blackwell, Cambridge, MA, 1985).

[41] C. Stolk and M. de Hoop, Wave Motion **43**, 579 (2006).

[42] M. Fink, W. A. Kuperman, J.-P. Montagner, and A. Tourin, *Imaging of Complex Media with Acoustic and Seismic Waves* (Springer-Verlag, Berlin, 2002).

[43] J.-P. Fouque, J. Garnier, G. Papanicolaou, and K. Solna, *Wave Propagation and Time Reversal in Randomly Layered Media* (Springer, New York, 2007).

[44] G. Beylkin, J. Math. Phys. **26**, 99 (1985).